Article

Metal Modified NaY Zeolite as Sorbent for the Ultra-Deep Removal of Thiophene in Simulated Coke Oven Gas

Fanjing Wei [1,2], **Xiaoqin Guo** [1,2], **Weiren Bao** [1,2], **Liping Chang** [1,2,*] **and Junjie Liao** [1,2,*]

[1] State Key Laboratory of Clean and Efficient Coal Utilization, Taiyuan University of Technology, Taiyuan 030024, China; fanjingwei321@163.com (F.W.); 18435180475@163.com (X.G.); baoweiren@tyut.edu.cn (W.B.)

[2] Key Laboratory of Coal Science and Technology, Ministry of Education, Taiyuan University of Technology, Taiyuan 030024, China

[*] Correspondence: lpchang@tyut.edu.cn (L.C.); liaojjie@163.com or liaojunjie@tyut.edu.cn (J.L.)

Abstract: The ultra-deep removal of thiophene is essential for the conversion of coke oven gas to methane and metal modified Y zeolite has excellent thiophene adsorption capacity. The effects of temperature on chemisorption between metal modified Y zeolite and thiophene and the reductive gases in coke oven gas on the thiophene adsorption performance still remains ambiguous. To address the aforementioned aims, series of NaMY (M = Ce, Ni, Zn and Ag) were prepared via ion-exchanged with Na^+ of NaY, and two comparable sets of thiophene adsorption evaluation were conducted in a fixed bed reactor: (1) NaY and NaMY were evaluated at different temperatures in simulated coke oven gas, and (2) NaCeY was evaluated in N_2 and different reductive atmospheres. The results show that NaNiY, NaZnY and NaAgY could adsorb thiophene via π-complexation, however, NaCeY mainly through S-Ce bond. Π complexation becomes weak above 150 °C, and the strength of S-Ce bond varies little when the temperature rises to 250 °C. Compared with that of other sorbents, the breakthrough adsorption capacity for thiophene ($Q_{b\text{-thiophene}}$) of NaAgY reaches the highest 144 mg/g at 100 °C, but decreases sharply when temperature rises to 200 °C. NaCeY has relatively low variation in $Q_{b\text{-thiophene}}$ from 100 °C to 200 °C. Moreover, Ce(IV) in NaCeY is more favorable for thiophene adsorption than Ce(III) in coke oven gas and the presence of H_2 and CO would reduce the desulfurization activity of NaCeY. For the industrial utilization of thiophene ultra-deep removal, NaAgY has an excellent potential below 150 °C, while NaCeY with more Ce(IV) has a good prospect at 150–250 °C.

Keywords: coke oven gas; thiophene; adsorption; Y zeolite; metal modification

1. Introduction

Coke oven gas (COG), rich in H_2 (55–60%), CH_4 (23–27%) and CO (5–8%), is the main byproduct of the coking industry, and the annual production of COG in China is approximately 180 billion m^3 in recent years [1,2]. COG is sought as an important fuel and chemical raw material, and methane synthesis is one of the most important ways in which it can be used effectively [1,3,4]. COG also contains a variety of sulfur-containing and nitrogen-containing compounds, and it needs to be removed by pretreatment and fine desulfurization prior to methane synthesis [5]. Tar, naphthalene, benzene, ammonia and H_2S in COG could be efficiently removed through pretreatment. Organic sulfides COS, CS_2 and thiophene in COG can be converted into H_2S through primary and secondary hydrogenation through fine desulfurization, and then H_2S could be effectively absorbed and eliminated by metal oxides [6–10]. After fine desulfurization, COS and CS_2 are almost completely eliminated, and thiophene can just be removed to ppmv level because of its high chemical stability and low chemical reaction rate by hydrodesulfurization technology [11–14], whereas the presence of ppmv thiophene in COG can lead to the irreversible poisoning of Ni-based methanation catalyst, thereby shortening catalyst

life, reducing methane production and increasing economic costs [1,3,15]. To meet the stringent requirements of thiophene concentration for methane synthesis, thiophene should be reduced to below 0.1 ppmv or even eliminated before the methanation process, therefore the ultra-deep removal of thiophene in COG has become an urgent problem to be solved.

In recent years, methods for ultra-deep removal of thiophene have been developed, and adsorption method with the advantages of high desulfurization accuracy and thiophene adsorption capacity has received widespread attention [16–19]. NaY zeolite exhibits excellent thiophene removal performance and has been widely used in the field of liquid fuel desulfurization [20]. Previous research has shown that metal modification over NaY zeolite can significantly improve the thiophene adsorption capacity [21–26]. Oliveira et al. [27] studied the adsorption capacity for thiophene in isooctane over NiY, ZnY and AgY, and the results show that the adsorption capacity for thiophene at 30 °C follows the order AgY > NiY > ZnY, and it changes at 60 °C following that AgY > ZnY > NiY. In the presence of aromatics and olefins in isooctane solution, the adsorption capacity for thiophene of studied sorbent will decrease notably [27]. The results were also observed by Zhang et al. [28] in the study of dibenzothiophene removal over various ion-exchanged NaY zeolites in n-octane solutions at 60 °C. Lin et al. [29] presented results of the adsorption behavior of AgY and CeY for thiophene in n-heptane solutions at 25 °C, which indicated CeY has better desulfurization performance than AgY. Song et al. [23] used the AgY and CeY zeolites for adsorption of thiophene in model gasoline at 50 °C and the results show that the capacity for sulfur removal with model gasoline containing only thiophene and benzothiophene has an order ranking of AgY > CeY, whereas, for any of the aromatics, nitrogen, and olefins that exist in model gasoline, the order is changed: CeY > AgY. The similar conclusion was reported by Han et al. [30] based on the adsorption removal of thiophene over NiY zeolite in hexene and toluene solutions at ambient temperature. As a summary, NiY, CeY, ZnY and AgY zeolite has good thiophene adsorption capacity in a liquid fuel system, and the presence of aromatic, hydrocarbon and nitrogenous compounds in feedstock has a negative impact on the thiophene adsorption capacity of metal modified Y zeolite. Most of the previous studies on the adsorption desulfurization of thiophene over metal modified Y zeolite have focused on liquid fuel desulfurization, and there is little research on the adsorptive desulfurization of thiophene in COG.

The working conditions of thiophene adsorption in COG and liquid fuel systems are quite different, and metal modified Y zeolite used for ultra-deep removal of thiophene in COG mainly faces two problems that need to be clarified: (1) in a liquid fuel system, the desulfurization temperature ranges from ambient temperature to about 60 °C [27,29]. In order to accommodate the methane synthesis process, the desulfurization temperature usually ranges from 100 °C to 250 °C in COG. The chemisorption between metal modified Y zeolite and thiophene is easy to be desorbed at relatively high temperature, and it is essential to investigate the effect of temperature on the thermal stability of chemisorption. (2) Components of the feedstock may negatively affect the thiophene adsorption properties of Y zeolite [23]. Aromatic, hydrocarbon and nitrogenous compounds in gasoline feedstock can greatly decrease the thiophene adsorption of metal modified Y zeolite [27,28]. The effect of large amounts of reductive gases H_2 and CO in COG on the thiophene adsorption performance of metal modified Y zeolite remains unclear. Meanwhile, the reductive gases will change the valence state of metal in Y zeolite. The Ce of NaCeY prepared by this method mentioned above exists in the form of Ce(IV), and the reductive gases would convert Ce(IV) into Ce(III), thereby affecting the thiophene adsorption capacity of NaCeY. Therefore, the effect of Ce valence states in NaCeY on the adsorption capacity of thiophene needs to be further investigated.

To solve the first problem mentioned above, series of NaCeY, NaNiY, NaZnY and NaAgY were prepared from NaY by ion-exchanged method and subsequently used for adsorptive desulfurization of thiophene in simulated COG at 100 °C and 200 °C. On this basis, the chemisorption between thiophene and Y zeolite and their thermal stability were investigated by in situ FT-IR. For the second question above, the effect of reductive gases on

the adsorption performance of NaCeY was investigated by evaluating NaCeY in H_2/CO containing atmosphere and N_2 atmosphere. A set of NaCeY sorbents, containing different Ce valence states, was prepared and evaluated in N_2 atmosphere to investigate the effect of Ce valence state on the thiophene adsorption capacity of NaCeY.

2. Experimental Section

2.1. Sample Preparation

NaY zeolite was purchased from Nanjingheyi Chemical Co. Ltd., and they were ground to 0.180–0.425 mm before use. Thiophene, with purity higher than 99.5%, was purchased from Alfa Aesar Co. Ltd., USA. $Ce(NO_3)_3 \cdot 6H_2O$, $Ni(NO_3)_2 \cdot 6H_2O$, $Zn(NO_3)_2 \cdot 3H_2O$ and $AgNO_3$ with purity higher than 99.0% were all supplied by Aladdin Co. Ltd., Shanghai, China.

First, 10.000 g NaY was treated with 0.1 mol/L 100 mL metal nitrate solution (M=Ce, Ni, Zn, Ag) in a three-neck flask, and kept at 100 °C for 4 h with stirring under condensation reflux. Then, the sample was separated by filtration and washed by deionized water. In order to ensure that the metal nitrates not involved in ion exchange were completely washed away, the sample was washed 10 times with about 150 mL deionized water for each time, and the pH value of the filtered deionized water was ensured to be around 7. After that, the sample was dried at 120 °C for 4 h, and calcined at 550 °C for 4 h in air. NaY zeolite after metal modification was denoted as NaMY. For the Y zeolite after desulfurization, it was denoted as NaMY$_S$.

2.2. Desulfurization Instruments and Procedure

The sorbent was evaluated in a 680 mm × φ6.00 mm fixed bed reactor. Prior to desulfurization, sorbent was calcined at 350 °C for 3 h in a muffle furnace to remove the adsorbed water in sorbent, and then cooled to ambient temperature in a closed desiccator. The FT-IR spectra of NaY and NaMY sorbents during activation at 350 °C are shown in Figure S1 in the Supplementary Materials, and it can be seen that the adsorbed water in sorbent can be removed after being calcined at 350 °C. The desulfurization equipment is shown in Figure 1. Firstly, 0.80 g NaY or NaMY was placed in the fixed bed reactor. Afterwards, the furnace was heated to 100 °C or 200 °C. The thiophene stream was taken out through Ar flow (1.5 mL/min) and then met with simulated COG (115 mL/min). The liquid thiophene in a container was precisely controlled by a cooling water recycling system with an inlet thiophene concentration of 300 ppmv (1.14 mg/L). The space velocity was 5500 h^{-1} during the thiophene removal process. Table 1 lists the composition of the simulated COG. The thiophene adsorption performances of NaY and NaMY sorbents were evaluated through online measurement of thiophene concentration at the outlet by an HPR-20 QIC mass spectrometer (MS) (Hiden, Warrington, UK). The sorbent was considered to be breakthroughed when the thiophene concentration reached 0.1 ppmv (0.00038 mg/L). The breakthrough adsorption capacity for thiophene of sorbent was used to estimate the sorbent desulfurization performance, and it was calculated using the following Equation (1).

$$Q_{\text{b-thiophene}} = \frac{\int_0^t q(c_1 - c)dt}{1000m} \tag{1}$$

where, $Q_{\text{b-thiophene}}$ (mg/g) was the breakthrough adsorption capacity for thiophene of sorbent; t (min) was the breakthrough time; q (mL/min) was the total gas flow; c_1 and c (mg/L) were the inlet and outlet thiophene concentration, respectively; m (g) was the sorbent weight.
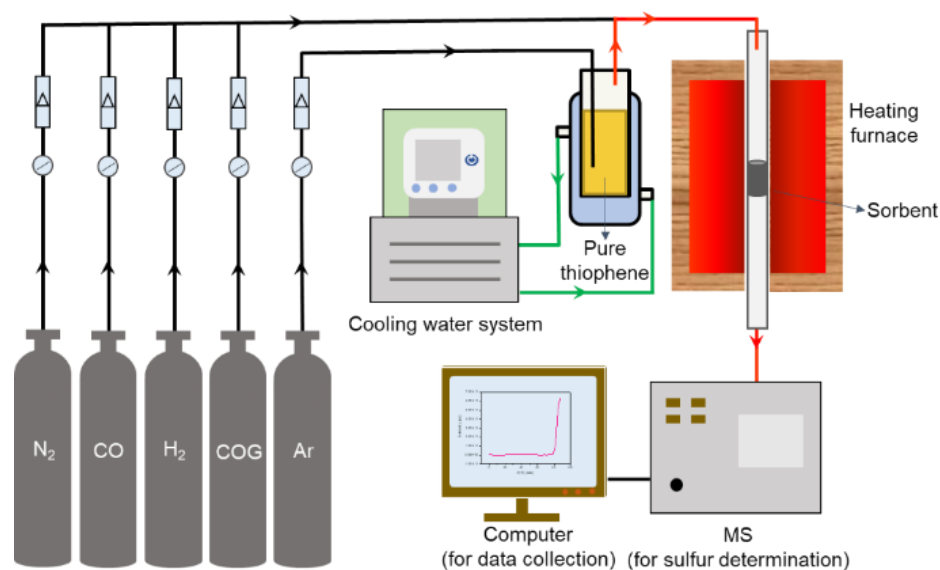
Figure 1. Schematic of equipment for thiophene removal.

Table 1. Composition of simulated COG.

Gas	H_2	CH_4	CO	N_2	CO_2	O_2
Content (vol%)	58.77	26.70	8.09	3.58	2.04	0.82

The precise determination of thiophene concentration has a large impact on the accuracy of sorbent desulfurization evaluation. Therefore, obtaining the relationship between thiophene concentration and its signal in MS is the basis for the accuracy of this study. We reported detailed steps to obtain the thiophene concentration from its signal value in a previous study [4].

According to different purposes of desulfurization, atmospheres can be changed. In order to study the effect of desulfurization atmospheres on thiophene adsorption capacity of sorbent, COG can be replaced by other gases for evaluation, including $8CO + 92N_2$ (vol%), $59H_2 + 41N_2$ (vol%) and N_2. To investigate the effect of the chemical valence of Ce on desulfurization performance, the following experiments were designed: Four copies of NaCeY sorbent were pretreated under four conditions for 3 h: 200 °C in H_2, 600 °C in H_2, 200 °C in CO and 200 °C in $H_2 + CO$ (Ar is equilibrium gas, H_2 or CO content is 10 vol%). The pretreated conditions were labelled as H_{2-200}, H_{2-600}, CO_{-200} and $H_2 + CO_{-200}$, respectively. NaCeY sorbent after pretreated under four kinds of conditions was evaluated in N_2 atmosphere.

2.3. Characterization of Sorbent

TG-DTG curves of sorbent were obtained using a STA 449 F3 thermal analyzer (NET-ZSCH, Germany). A roughly 10 mg sample was exposed to a heating rate of 5 °C/min from 40 °C to 800 °C under a continuous flow of air (50 mL/min).

The surface area and pore structure of sorbent were analyzed by N_2 adsorption-desorption at −196 °C on an ASAP 2460 apparatus (Micromeritics, USA). Prior to analysis, the fresh sample was evacuated at 300 °C for 3 h. Total specific surface area, micropore specific surface area and pore volume were calculated by BET, t-plot and DFT methods, respectively.

XRD analysis was measured using a Mini Flex 600 spectrometer (Rigaku, Japan) with Cu-Kα radiation at 40 kV and 100 mA. During the measurement, the scanning rate is 5°/min with the 2θ range of 5–35°.

The element contents in the sorbent were analyzed by a SPETRO ARCOS inductively coupled plasma optical emission spectrometer (ICP-OES) (Spike, Karlsruhe, Germany). Firstly, 0.05 g NaY or NaMY sorbent and 1.0 g potassium hydroxide were put into a crucible and mixed evenly. It was then calcinated in a muffle furnace at 650 °C for 1 h and cooled to ambient temperature. Finally, the mixture after calcination was dissolved with dilute nitric acid for determination. The exchange degree of Na$^+$ during the ion exchange process was calculated using the following Equation (2).

$$E_{\mathrm{Na}}(\%) = 100 \times (n_{\mathrm{NaY}} - n_{\mathrm{NaMY}})/n_{\mathrm{NaY}} \tag{2}$$

where E_{Na} (%) was the exchange degree of Na$^+$; and n_{NaY} and n_{NaMY} (mmol/g) were the Na content in parent NaY and NaMY zeolite, respectively.

FT-IR characterization of fresh and spent sorbent was conducted with a INVENIO R FT-IR spectrometer (Bruker, Karlsruhe, Germany). The scanning ranges from 400 cm^{-1} to 4000 cm^{-1} with a resolution of 4 cm^{-1}. Then, 1.0 mg of sorbent was mixed with 100 mg of KBr and ground well to make a tablet prior to FT-IR.

In situ FT-IR of thiophene adsorption on sorbent surface was characterized by a FT-IR spectrometer mentioned above. Firstly, 20 mg sorbent was made into a wafer with the diameter of 13 mm and placed in a cell. The in situ FT-IR characterization contained the following three steps: (1) The wafer was pretreated (6.0×10^{-5}–7.0×10^{-5} Pa) at 550 °C for 1 h in air to desorb the impurities such as moisture and CO$_2$ in sorbent. (2) After cooling to ambient temperature, the wafer was treated in Ar atmosphere to 350 °C with 5 °C/min heating rate and then cooled by water recycling. Infrared spectra at different temperatures were collected during the cooling process. (3) Thiophene saturated steam was adsorbed on sorbent under a high vacuum with a pressure less than 1.0×10^{-5} Pa for 0.5 h at ambient temperature, and then the temperature-processed desorption was carried out under vacuum condition. Infrared spectra of sorbents were collected with 10 °C/min heating rate from room temperature to 350 °C.

3. Results and Discussion

3.1. Effects of Temperature on Desulfurization Performance of Metal Modified Y Sorbent

3.1.1. Thiophene Adsorption Capacity of Sorbent

Thiophene breakthrough adsorption curves and $Q_{\text{b-thiophene}}$ of NaY, NaCeY, NaZnY, NaNiY and NaAgY sorbents in simulated COG at different temperatures are shown in Figure 2a–d. When the desulfurization temperature is 100 °C, the $Q_{\text{b-thiophene}}$ of different metal modified Y zeolites is higher than that of NaY (Figure 2b), indicating that metal modification can significantly improve the desulfurization performance of NaY. The $Q_{\text{b-thiophene}}$ of different metal modified Y zeolites follows the order: NaAgY >> NaZnY > NaNiY > NaCeY > NaY. NaAgY sorbent has the highest $Q_{\text{b-thiophene}}$, about 144 mg/g, while NaCeY has the lowest $Q_{\text{b-thiophene}}$ among the four metal modified Y zeolites.

Notably, the order of $Q_{\text{b-thiophene}}$ changes significantly at 200 °C: NaCeY >> NaNiY > NaAgY > NaY > NaZnY (Figure 2d). When the temperature increases to 200 °C, the $Q_{\text{b-thiophene}}$ of NaNiY and NaZnY sorbents are almost 20 times less than that of 100 °C, and the $Q_{\text{b-thiophene}}$ of NaAgY sorbent decreases to about one fiftieth of that at 100 °C. In contrast, the $Q_{\text{b-thiophene}}$ reduction of NaCeY sorbent is not obvious, indicating that the adsorption performance of NaCeY adsorbent for thiophene is less affected by temperature.
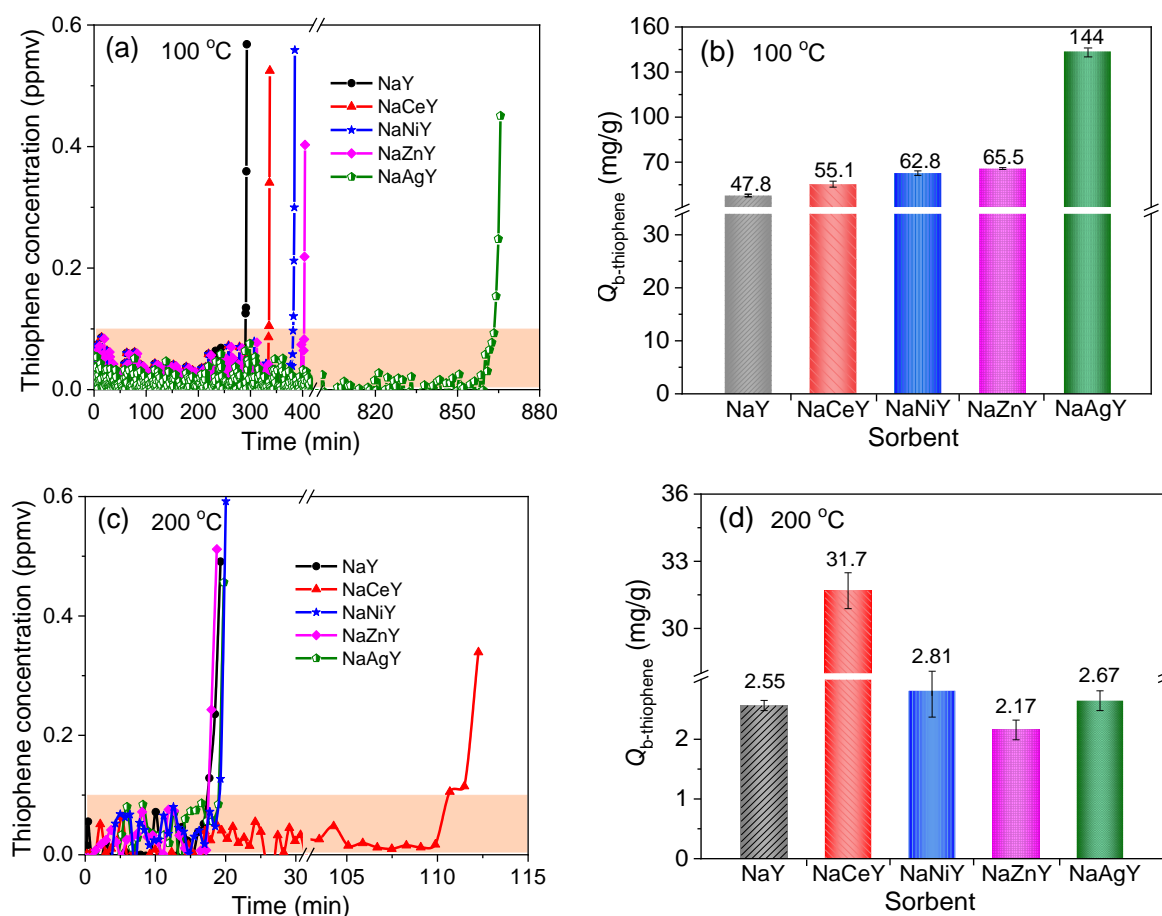
Figure 2. Thiophene breakthrough adsorption curves (**a**,**c**) and $Q_{b\text{-thiophene}}$ (**b**,**d**) of different Y zeolites at 100 °C and 200 °C in simulated COG.

Table 2 presents the thiophene adsorption capacities of Y zeolites in different systems in the literature. The thiophene adsorption capacity of Y zeolite varies greatly when the feedstock, initial thiophene concentration, temperature conditions are different. From the studied results in the literature, it can be seen that the adsorption capacity of Y zeolite to thiophene ranges from 5.39 mg/g to 394 mg/g [27,31]. In this work, the thiophene adsorption capacities of NaAgY and NaCeY in simulated COG are still 114 mg/g and 31.7 mg/g, which may have certain potential for industrial application.

Table 2. A comparison of thiophene adsorption capacity of different Y zeolites at various conditions.

Sample	Feedstock	Initial Thiophene Concentration (ppm)	Conditions	Thiophene Capacity of Sorbent (mg/g)	Reference
NaY				199	
ZnY	Isooctane	200	Static adsorption at 60 °C for 12 h	313	[27]
NiY				302	
AgY				394	
AgY	n-heptane	700	Dynamic adsorption at 25 °C	28.9	[29]
CeY				35.9	
CeY	Benzene	600	Static adsorption at 25 °C for 24 h	5.39	[31]
NaAgY	Simulated COG	300	Dynamic adsorption at 100 °C	144	This work
NaCeY			Dynamic adsorption at 200 °C	31.7	

3.1.2. Composition and Structure Analysis of Sorbent

The thiophene adsorption capacities of different NaMY sorbents in simulated COG show a great difference with the increase of temperature. There are many factors affecting the thiophene adsorption capacity of sorbent, the differences in the sorbent structure may be one of the factors. In NaY zeolite framework, the [SiO$_4$] tetrahedron is electrically neutral and the [AlO$_4$] tetrahedron carries one unit of negative charge [32]. Therefore, aluminosilicate zeolite composed of Si and Al atoms have an anionic framework structure, which needs to be equilibrated with Na$^+$ in the vicinity of negatively charged [AlO$_4$]$^-$ (Figure 3). After Ag$^+$ is ion-exchanged with NaY, the generally accepted model is that Na$^+$ in NaY is replaced by Ag$^+$. Some studies show that after the ion exchange of the higher-charged cations such as Ni^{2+}, Ce^{4+} with NaY, Na$^+$ is finally probably replaced by [NiOH]$^+$, [Ce(OH)O]$^+$ [33,34]. During the ion exchange process, part of the structure of metal modified Y zeolite would be destroyed due to the charge balance during metal modification process [35,36].
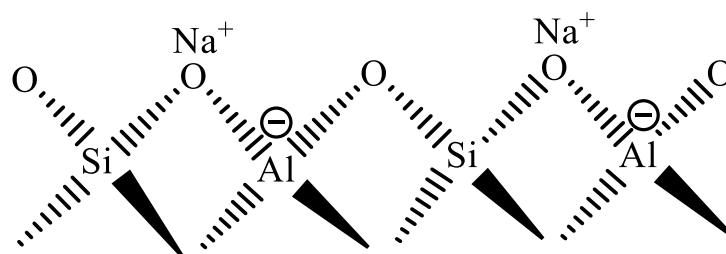

Figure 3. Schematic diagram of the structure of NaY zeolite.

To study the thermal stability of different Y zeolites, TG analysis was conducted. As can be seen in Figure 4a, the weight loss of NaY and NaMY sorbents is between 20% and 25% during the heating process. DTG curves of different Y zeolites in Figure 4b have distinct weight loss peaks before 300 °C, which is attributed to the adsorbed moisture in Y zeolite [36–38]. The abundant micropores and OH groups in NaY and NaMY can easily absorb moisture in air. After 300 °C, the weight of Y zeolite changes little, indicating that the chemical structure of Y zeolite prepared after calcination is relatively stable.
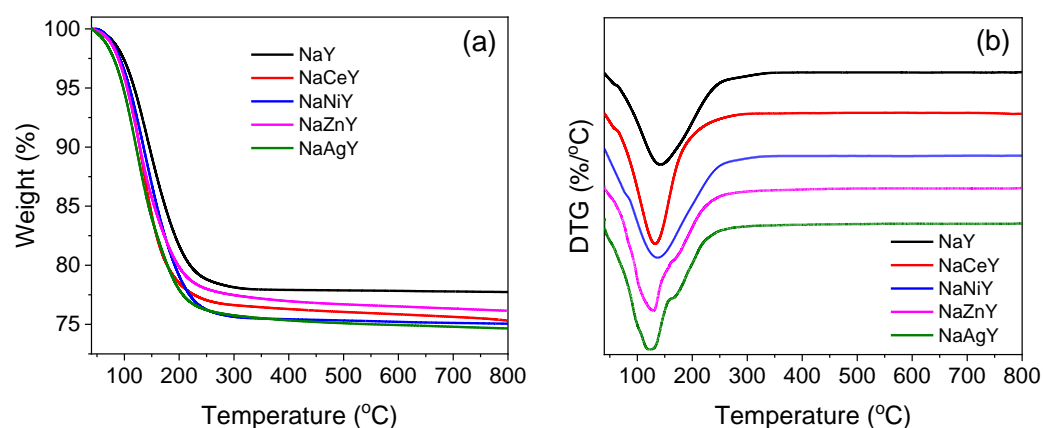

Figure 4. TG (**a**) and DTG (**b**) curves of different Y zeolites.

N$_2$ adsorption and desorption isotherms of NaY and NaMY sorbents show that the curves increase rapidly at low p/p$_0$ and then rise slowly at high p/p$_0$ (Figure 5a). The N$_2$ adsorption curve is typical of type I adsorption isotherm, implying NaY and NaMY sorbents have micropore structure. The pore size of sorbents ranges from 0.5 nm to 1.2 nm (Figure 5b). Table 3 shows the pore structure parameters of sorbents. Compared with that of NaY sorbent, the BET surface area and micropore volume of metal modified Y zeolite

have a slight decrease. Notably, the most available pore size (a_0) of NaCeY sorbent is bigger than that of other sorbents, which may be due to changes of pore structure caused by desiliconization and dealumination during the ion exchange process.
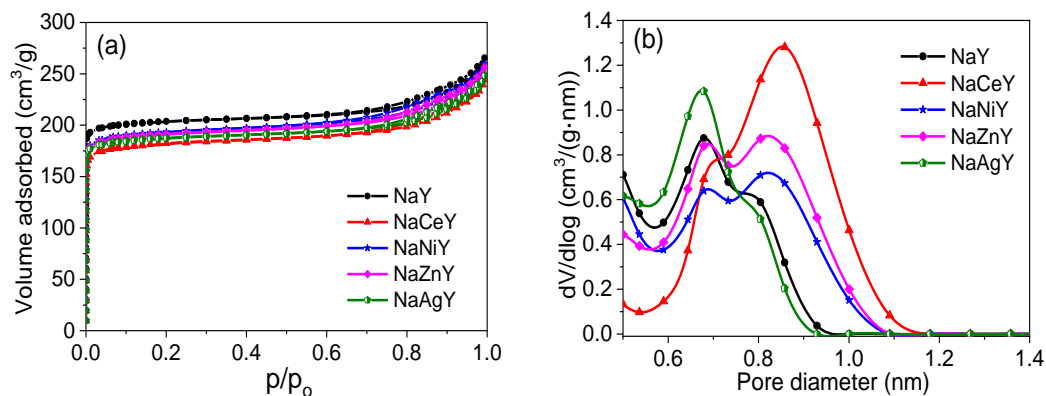

Figure 5. N_2 adsorption and desorption isotherms (**a**) and pore size distribution (**b**) of different Y zeolites.

Table 3. Surface area, micropore volume and the most available pore size (a_0) of different Y zeolites.

Sample	S_{BET} (m^2/g)	S_{micro} (m^2/g)	V_{micro} (cm^3/g)	a_0 (nm)
NaY	834	789	0.30	0.68
NaCeY	735	682	0.26	0.80
NaNiY	783	724	0.27	0.73
NaZnY	775	721	0.27	0.73
NaAgY	766	719	0.27	0.64

In order to study the crystal structure of different Y zeolites, the XRD characterization was performed. Figure 6a shows the XRD patterns of fresh NaY and NaMY sorbents. Diffraction peaks at 10.21°, 11.97°, 15.73°, 18.76°, 20.44°, 23.76°, 27.14° and 31.49° belong to (220), (311), (331), (333), (440), (533), (642) and (555) crystal faces of Y zeolite, respectively [34,36,39,40]. It can be seen from Figure 6a that the crystal structure of NaNiY, NaZnY and NaAgY does not change significantly. For NaCeY sorbent, the (220) and (311) crystal faces disappear, which suggests that ion exchange with Ce could destroy part of the crystal faces of Y zeolite.
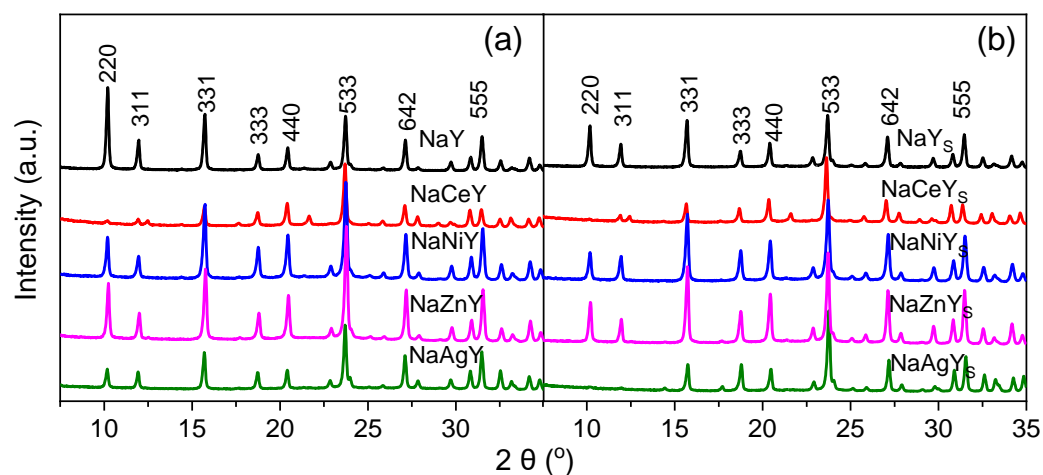

Figure 6. XRD patterns of Y zeolites before (**a**) and after (**b**) desulfurized in simulated COG at 100 °C.

The XRD patterns of the spent sorbents (Figure 6b) show that the crystal structures of the spent NaCeY, NaNiY and NaZnY sorbents were almost unchanged. However, the (220) and (311) crystal faces of spent NaAgY disappear, probably because thiophene covers the (220) and (311) crystal faces during the desulfurization process.

ICP characterization was conducted to determine the element contents of different sorbents. The characterization results (Table 4) show that the Si and Al contents in NaMY sorbent decrease after metal modification. The lowest amount of Si and Al in NaCeY demonstrates that Ce would cause desiliconization and dealumination of NaY during metal modification process, which is consistent with the literature [35,36,41]. After metal modification, Na content reduces from 3.78 mmol/g to approximately 3.2 mmol/g. The E_{Na} ranges from 12.4% to 17.7% and these values are lower than that in the literature [36,38], which may be caused by nitrate solution concentration, low exchange temperature and short exchange time. The order of loading metal contents in sorbents is as follows: Ag > Zn > Ni > Ce. The contents of Ni and Ce are about 0.5 mmol/g, and Zn and Ag are relatively higher (approximate 0.7 mmol/g). Combining the results of thiophene adsorption capacity and metal element content (Figure 2d and Table 4), it is found that there is no correlation between the contents of loading metals and $Q_{b\text{-thiophene}}$, probably due to the low contents of loading metals.

Table 4. Elemental contents and E_{Na} of different Y zeolites.

Sample	Element Content (mmol/g)				E_{Na} (%)
	Si	Al	Na	M	
NaY	10.4	3.44	3.78	-	-
NaCeY	9.58	3.24	3.31	0.505	12.4
NaNiY	10.2	3.34	3.23	0.519	14.6
NaZnY	10.4	3.41	3.13	0.692	17.2
NaAgY	9.72	3.28	3.11	0.723	17.7

Note: M represents Ce, Ni, Zn and Ag; E_{Na} denotes the exchange degree of Na^+.

From the above analysis, we can conclude that the crystal structure and metal content of NaMY sorbent are not the main factors affecting its thiophene adsorption capacity. The difference in the chemisorption mode and thermal stability between thiophene and NaMY sorbent may be the fundamental reason for the difference in thiophene adsorption capacity of sorbent at different temperatures.

3.1.3. Thermal Stability of Chemisorption between Thiophene and Sorbent

In general, the chemisorption between thiophene and metal ions has two modes: π-complexation and S-M bond [21,27,42]. To study the chemisorption mode of thiophene over different metal modified Y zeolites, FT-IR characterization of fresh and spent NaY and NaMY sorbents was conducted and the results are shown in Figure 7a,b. The peaks at 3450 cm^{-1} and 1640 cm^{-1} are assigned to the OH groups in H_2O molecules [43], which is caused by the adsorbed moisture in air during the grinding process before FT-IR characterization. Peaks in the range of 900–1200 cm^{-1} are assigned to Si-O-Si groups in Y zeolite [5]. Compared with that of fresh sorbents, some new peaks appear in FT-IR spectra of spent sorbents. For NaY$_S$, NaCeY$_S$, NaNiY$_S$, NaZnY$_S$ and NaAgY$_S$ sorbents, the peak at 1401 cm^{-1} is assigned to the symmetric stretching of C=C bond of thiophene [44–46], indicating the presence of adsorbed thiophene in the spent sorbents (Figure 7b). In addition, a characteristic peak at 1385 cm^{-1} appears for all spent sorbents. Theoretically, if the adsorption of thiophene is achieved by the complexation between π electrons of thiophene ring and metal, the electron density across the thiophene ring will decrease, resulting in a red shift of C=C stretching bond [45,46]. Thus, the characteristic peak at 1385 cm^{-1} can be assigned to a red shift of 1401 cm^{-1}, and it reflects π-complexation between thiophene and metal ions. It is concluded that when the temperature is 100 °C, Y zeolites loaded with

Ce^{4+}, Ni^{2+}, Zn^{2+}, Ag^+ still have the ability to adsorb thiophene by π-complexation between metal ions and thiophene.
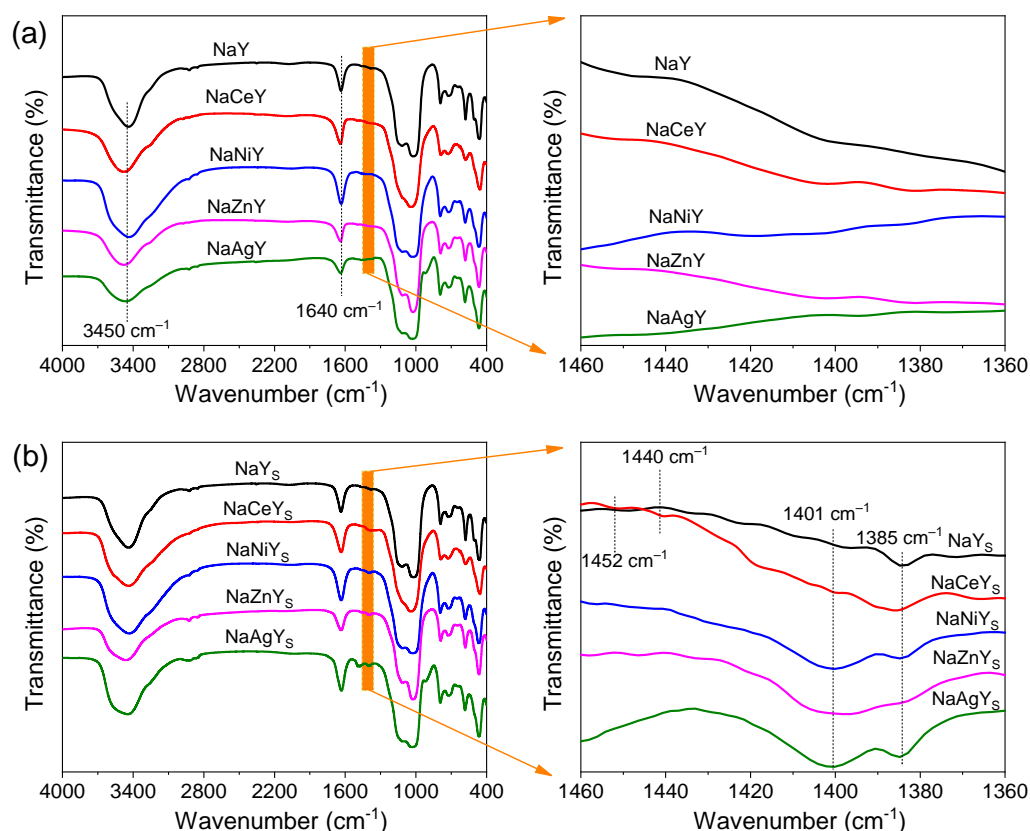

Figure 7. FT-IR spectra of Y zeolites before (**a**) and after (**b**) desulfurized in simulated COG at 100 °C.

If the sulfur atom of thiophene directly interacts with metal as a bond, the electron density of carbon atoms in thiophene will increase, leading to a blue shift of C=C stretching [45,46]. Therefore, the peak at 1452 cm^{-1} is assigned to the blue shift of 1401 cm^{-1}, and it reflects chemisorption of S-M bond. The peak at 1440 cm^{-1} is assigned to the stretching vibration of S-Ce bond [47]. For NaCeY$_S$ sorbent, the appearance of peaks at 1452 cm^{-1} and 1440 cm^{-1} proves the existence of S-Ce bond in NaCeY$_S$ sorbent (Figure 7b), indicating that Ce ion in Y zeolite could also adsorb thiophene via a direct S-Ce bond. Ni^{2+} in NaNiY zeolite can adsorb thiophene via S-Ni bond, which is observed at room temperature [48]. In this work, NaNiY$_S$ sorbent has no characteristic peak of 1452 cm^{-1}, implying that in coke oven gas S-Ni bond almost disappears at 100 °C.

The characteristic peak intensity of π-complexation of NaAgY is significantly stronger than that of the other sorbents (Figure 7b), indicating that the thiophene content in NaAgY is higher than that of the other sorbents, and this result is consistent with the $Q_{b\text{-thiophene}}$ of sorbent. The $Q_{b\text{-thiophene}}$ of NaNiY, NaZnY and NaAgY is higher than that of NaCeY at 100 °C, implying that π-complexation is significantly more effective than the S-Ce bond for thiophene adsorption at 100 °C. However, NaCeY has much higher $Q_{b\text{-thiophene}}$ than the other sorbents at 200 °C, which suggests that thiophene absorbed via π-complexation would be easily desorbed and via S-Ce bond is relatively hard to be desorbed.

Since the chemisorption between NaCeY and thiophene has both π-complexation and S-Ce bond, NaCeY was selected to further study the thermal stability of π-complexation and S-Ce by in situ FT-IR. The peak at 3102 cm^{-1} is assigned to the unsaturated C-H stretching vibration of thiophene ring [37]. As the desorption temperature increases, the peak of C-H stretching vibration shows an obvious red shift (Figure 8a). This indicates that

as the desorption temperature increases, the energy of C-H group in thiophene molecular becomes lower and the thiophene adsorbed on Y zeolite becomes more and more stable.
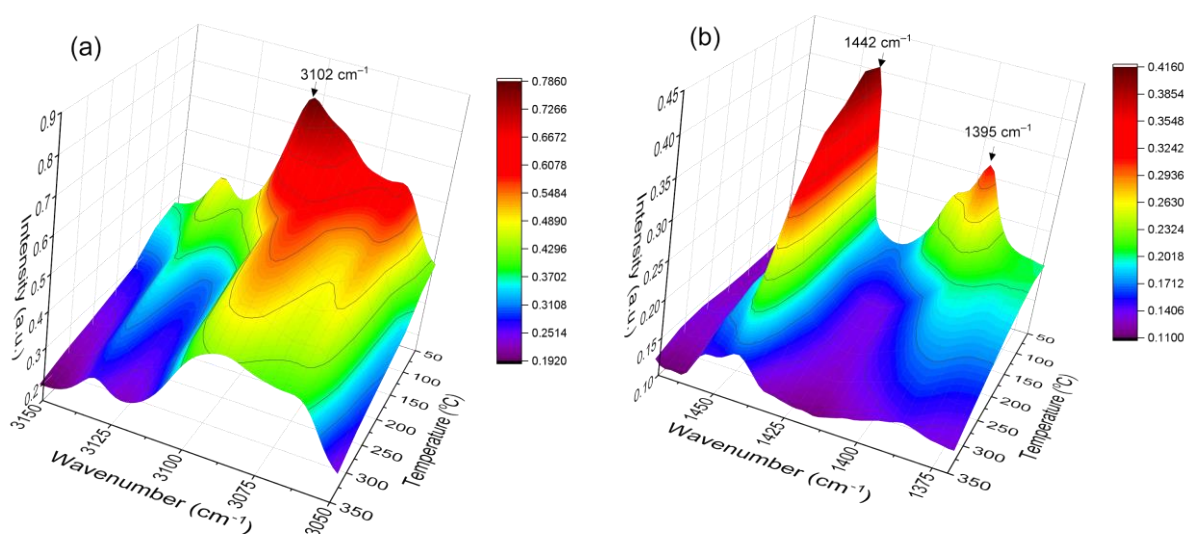

Figure 8. In situ FT-IR spectra of NaCeY$_S$ sorbent at different desorption temperatures in the regions of 3150–3050 cm^{-1} (**a**) and 1470–1370 cm^{-1} (**b**).

Previous research has shown that the peak at 1395 cm^{-1} is attributed to the C=C stretching vibration of thiophene adsorbed on NaCeY via π-complexation [45,46], while the peak at 1442 cm^{-1} is attributed to the stretching vibration of S-Ce bond [47]. Figure 8b shows that the peak intensity of S-Ce bond is much stronger than that of π-complexation, indicating that thiophene is mainly adsorbed on NaCeY via S-Ce bond. The peak at 1395 cm^{-1} becomes weak when the desorption temperature reaches 150 °C, suggesting that most of the thiophene adsorbed via π-complexation can be desorbed at 150 °C. The strength of stretching vibration of S-Ce bond changes little when the desorption temperature ranges from 50 °C to 250 °C, implying that thiophene adsorbed through S-Ce bond is difficult to desorb below 250 °C.

The big difference in the thiophene adsorption capacity of NaAgY and NaCeY at 100 °C and 200 °C is mainly caused by their different chemisorption modes and thermal stability. The thiophene adsorption over NaAgY and NaCeY is summarized in Figure 9. Thiophene can be adsorbed on Ag active site of Y zeolite via π-complexation, while on Ce ion mainly via S-Ce bond. The thermal stability of S-Ce bond is higher than that of π-complexation in the range of 100 °C to 200 °C. When the desulfurization temperature is 100 °C, the thiophene adsorption capacity of NaAgY is much higher than that of NaCeY due to the excellent thiophene adsorption capacity of Ag active site. With the increase of temperature, a large amount of thiophene on NaAgY is desorbed, while a small amount of thiophene adsorbed on NaCeY is desorbed. Therefore, the thiophene adsorption capacity of NaCeY is much higher than that of NaAgY when the desulfurization temperature is 200 °C.

According to Table 4, 1.0 ton NaCeY contains 505 mol Ce and 1.0 ton NaAgY has 723 mol Ag. Taking the Aladdin price as an example, the current prices of per mole Ce(NO$_3$)$_3$·6H$_2$O and AgNO$_3$ are about \$27.8 and \$411, respectively. The nitrate cost to manufacture 1.0 ton NaCeY and NaAgY are about \$14,039 (505 × 27.8) and \$297,153 (723 × 411), respectively, neglecting the loss of metal nitrate during the ion exchange process. It can be seen that the cost of AgNO$_3$ is about 20 times higher than that of Ce(NO$_3$)$_3$·6H$_2$O. On balance, NaCeY sorbent may have better industrial utilization prospects than NaAgY at relatively high temperature. The understanding of thiophene adsorption mechanism over NaCeY in coke oven gas may provide a theoretical basis for the targeted design of thiophene adsorption active sites in NaCeY zeolite.
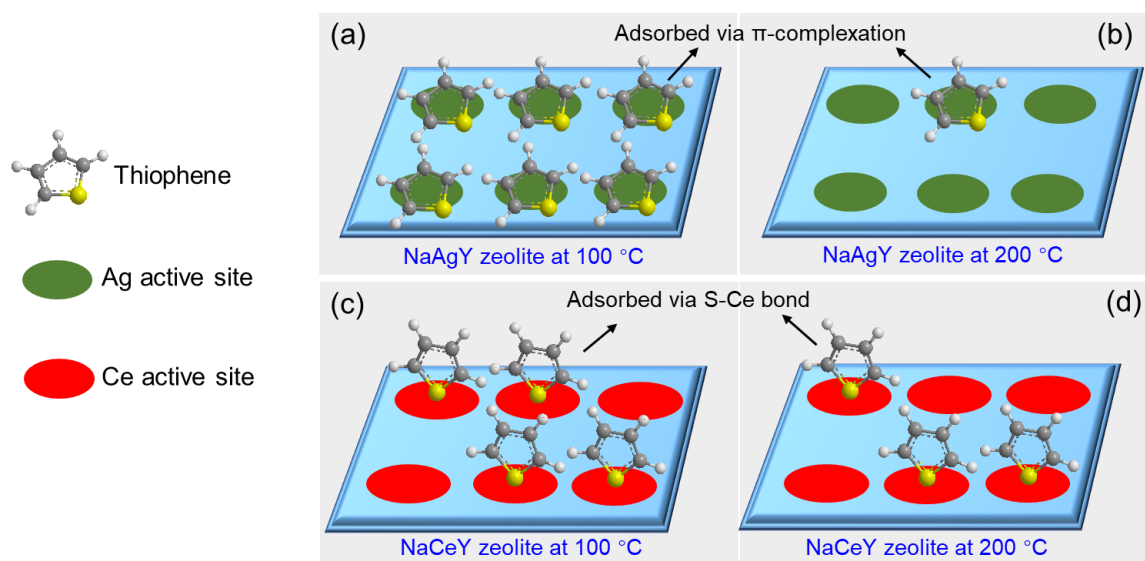
Figure 9. Thiophene adsorption over different NaMY sorbents. (**a**) NaAgY at 100 °C; (**b**) NaAgY at 200 °C; (**c**) NaCeY at 100 °C; and (**d**) NaCeY at 200 °C.

3.2. Desulfurization Performance of NaCeY Sorbent

3.2.1. Effects of Desulfurization Atmosphere on Thiophene Adsorption Capacity

The presence of reductive gases CO and H_2 in COG may change the chemical valence state of the active metals in sorbent, which in turn affects the thiophene adsorption capacity of sorbent. The XRD and element content results of sorbents (Figure 6a and Table 4) show that the chemical structure of NaCeY is more severely damaged than that of NaNiY, NaZnY and NaAgY. In other words, NaCeY has lower chemical stability compared with other NaMY sorbents, and the chemical valence state of Ce in NaCeY is easily changed during the desulfurization process. Therefore, NaCeY was chosen to study the effect of reductive gas in COG on the thiophene adsorption performance of NaMY sorbent.

NaCeY was evaluated in four kinds of atmospheres, and the thiophene breakthrough adsorption curves and $Q_{b\text{-thiophene}}$ of NaCeY are shown in Figure 10a,b, respectively. The $Q_{b\text{-thiophene}}$ of NaCeY sorbent is 57.6 mg/g in inert atmosphere N_2, while the $Q_{b\text{-thiophene}}$ of NaCeY decreases significantly in CO and/or H_2 containing atmosphere, and there is a more than 35% decrease in $Q_{b\text{-thiophene}}$. It suggests that the reductive atmosphere is not favorable for the adsorption of thiophene over NaCeY sorbent. NaCeY sorbent prepared in this work was obtained by calcining at 550 °C in air for 4 h, in which Ce exists in the form of Ce(IV). Generally, part of Ce(IV) in NaCeY will probably be converted into Ce(III) during desulfurization in reductive atmosphere, and the valence state of Ce may affect the thiophene adsorption performance of NaCeY.

3.2.2. Effects of Ce Valence State on Thiophene Adsorption Capacity

Due to the relatively low chemical stability of NaCeY, H_2 and CO in COG may reduce Ce(IV) to Ce(III) during the heating process. In order to determine the reduction temperature of Ce(IV) to Ce(III), H_2 and CO temperature-programmed reduction of NaCeY were conducted, respectively.
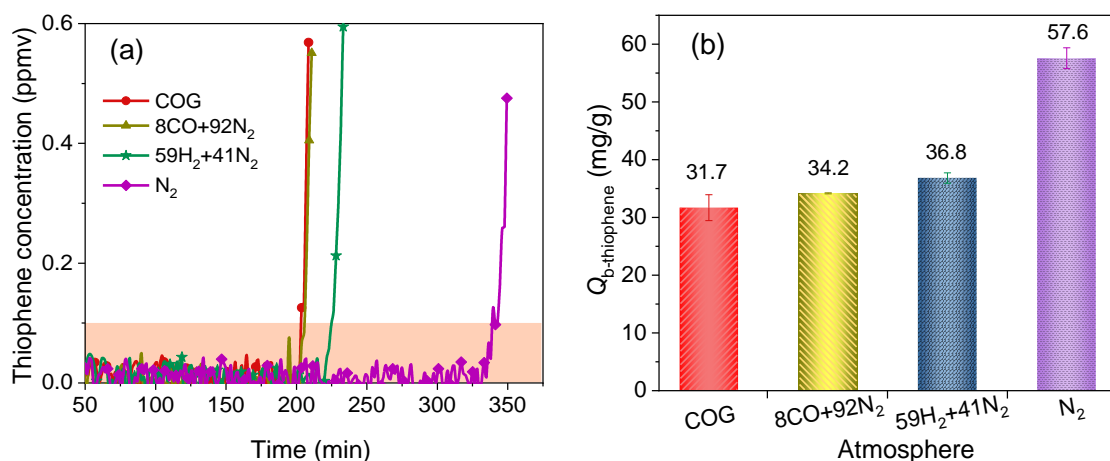
Figure 10. Thiophene breakthrough adsorption curves (**a**) and $Q_{b\text{-thiophene}}$ (**b**) of NaCeY in different desulfurization atmospheres at 200 °C.

As displayed in Figure 11a, a small peak of H_2 consumption occurs at around 200 °C, while H_2 consumption reaches a maximum at around 450 °C and disappears after 600 °C. H_2O is produced while H_2 is consumed. It indicates that the complete conversion of Ce(IV) species into Ce(III) in H_2 containing atmosphere is around 600 °C. Similar results have been observed in the literature, a reduction peak of H_2 can be observed at around 450–600 °C for NaCeY sorbent and this peak is assigned to the reduction of Ce(IV) species to Ce(III) species on the surface and in the supercage of zeolite [36]. The reduction of NaCeY in CO is shown in Figure 11b, CO content starts to decrease slowly from 150 °C, and its consumption reaches a maximum at 610 °C. At the same time, the product CO_2 was detected. The change in CO_2 content is exactly the opposite of that of CO. This suggests that CO is able to convert a small amount of Ce(IV) in NaCeY into Ce(III) starting from about 150 °C. Combined with the results of Ce reduction temperature, we can conclude that after being treated under H_{2-200}, CO_{-200} and $H_2 + CO_{-200}$ conditions, NaCeY contains a small amount of Ce(III). Under the condition of H_{2-600}, Ce(IV) in NaCeY sorbent can be completely converted into Ce(III).
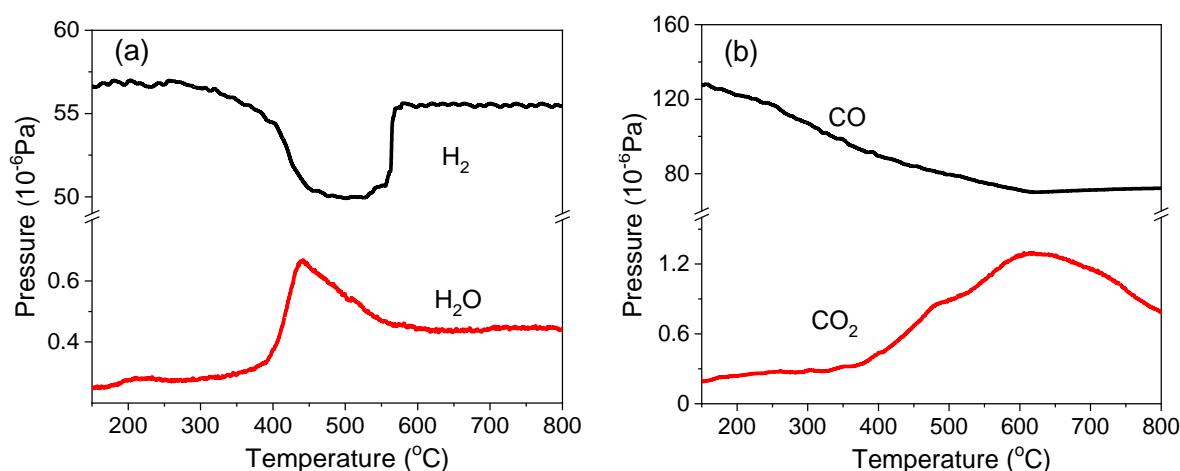

Figure 11. Reduction process of NaCeY sorbent in H_2 (**a**) and CO (**b**) containing atmospheres. Note that the data were obtained by follows: 0.05 g NaCeY was weight in a fixed bed reactor coupled with MS, and then was heated in $10H_2/CO + 90Ar$ (vol%) with a flow rate of 50 mL/min from ambient temperature to 800 °C with a heating rate of 2 °C/min.

The thiophene adsorption performance of NaCeY with different content of Ce(III) was evaluated in N_2 atmosphere, and thiophene breakthrough adsorption curves and $Q_{b\text{-thiophene}}$

of NaCeY are shown in Figure 12a,b, respectively. Compared with the $Q_{b\text{-thiophene}}$ of NaCeY containing totally Ce(IV) (57.6 mg/g, Figure 10b), the $Q_{b\text{-thiophene}}$ of NaCeY containing part of Ce(III) ranges from 13.6 mg/g to 19.0 mg/g. Significantly, the $Q_{b\text{-thiophene}}$ of NaCeY containing only Ce(III) is 4.96 mg/g, which is 8.61% of the highest $Q_{b\text{-thiophene}}$ of NaCeY. Therefore, it can be concluded that the adsorption capacity of Ce(IV) species in NaCeY for thiophene is much better than that of Ce(III).
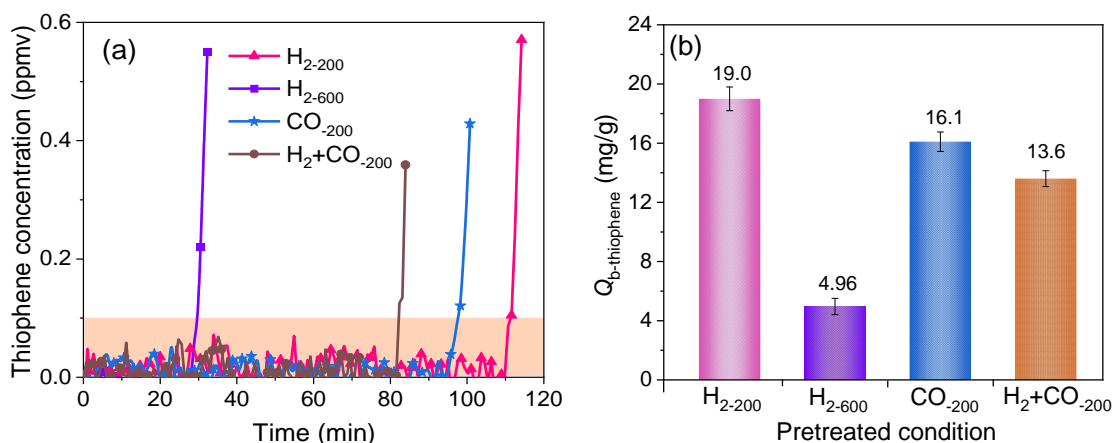

Figure 12. Thiophene breakthrough adsorption curves (**a**) and $Q_{b\text{-thiophene}}$ (**b**) of NaCeY sorbent pretreated at different conditions. (Desulfurization temperature is 200 °C; desulfurization atmosphere is N_2.).

4. Conclusions

The breakthrough adsorption capacity for thiophene in coke oven gas was successfully improved by metal (Ce, Ni, Zn and Ag) modification of NaY zeolite. At 100 °C, NaAgY has the highest breakthrough adsorption capacity for thiophene (144 mg/g), which is 1–2 times higher than NaZnY, NaNiY, NaCeY, and NaY. The thiophene adsorption capacities of NaNiY, NaZnY and NaAgY decrease remarkably from 100 °C to 200 °C, while the thiophene adsorption capacity of NaCeY is less affected by temperature. Thiophene is adsorbed via π-complexation on NaAgY sorbent, and mainly through S-Ce bond on NaCeY sorbent. π-complexation between thiophene and Y zeolite becomes weak above 150 °C, while the strength of S-Ce bond changes little until 250 °C. In addition, Ce(IV) species are more favorable for the adsorption of thiophene than Ce(III). The presence of H_2 and CO in coke oven gas can decrease the content of Ce(IV) of NaCeY, thereby reducing the desulfurization performance. Therefore, Ag modified Y zeolite would be a potential adsorbent for the ultra-deep removal of thiophene in coke oven gas below 150 °C, while Ce modified Y zeolite containing more Ce(IV) species has a promising application prospect at 150–250 °C.

Author Contributions: Conceptualization, L.C. and J.L.; methodology, W.B. and J.L.; validation, F.W. and J.L.; formal analysis, F.W.; investigation, X.G.; data curation, X.G.; writing—original draft preparation, F.W.; writing—review and editing, J.L.; supervision, L.C. and J.L.; project administration, J.L.; funding acquisition, J.L. All authors have read and agreed to the published version of the manuscript.

Data Availability Statement: Data available on request due to restrictions of privacy or ethical.

Conflicts of Interest: The authors declare no conflict of interest.

References

1. Qin, Z.F.; Zhao, Y.J.; Yi, Q.; Shi, L.J.; Li, C.M.; Yan, X.L.; Ren, J.; Miao, M.Q.; Xie, K.C. Methanation of coke oven gas over Ni-Ce/gamma-Al₂O₃ catalyst using a tubular heat exchange reactor: Pilot-scale test and process optimization. *Energy Convers. Manag.* **2020**, *204*, 112302. [CrossRef]
2. National Bureau of Statistics of China. *National Data 2020*; National Bureau of Statistics of China: Beijing, China, 2020.
3. Razzaq, R.; Li, C.; Zhang, S. Coke oven gas: Availability, properties, purification, and utilization in China. *Fuel* **2013**, *113*, 287–299. [CrossRef]
4. Khan, M.M.; Jin, L.; Khan, M.M.; Li, Y.; Saulat, H.; Zhang, Y.; Sarfraz, M.; Zhu, J.; Hu, H. CO₂ reforming of methane over activated carbon-Ni/MgO-Al₂O₃ composite catalysts for syngas production. *Fuel Process. Technol.* **2021**, *211*, 106595. [CrossRef]
5. Wei, F.; Guo, X.; Liao, J.; Bao, W.; Chang, L. Ultra-deep removal of thiophene in coke oven gas over Y zeolite: Effect of acid modification on adsorption desulfurization. *Fuel Process. Technol.* **2021**, *213*, 106632. [CrossRef]
6. Zhou, W.; Fan, F.; Chen, Z.; Zhou, A.; Zhang, Y.; Yao, F. A DFT investigation on the hydrodesulfurization mechanism of 4,6-dimethyldibenzothiophene over different Ni-Mo-S active sites via different direct desulfurization pathways. *Fuel* **2022**, *308*, 121971. [CrossRef]
7. Li, X.; Wang, X.; Wang, L.; Ning, P.; Ma, Y.; Zhong, L.; Wu, Y.; Yuan, L. Efficient removal of carbonyl sulfur and hydrogen sulfide from blast furnace gas by one-step catalytic process with modified activated carbon. *Appl. Surf. Sci.* **2022**, *579*, 152189. [CrossRef]
8. Frilund, C.; Simell, P.; Kurkela, E.; Eskelinen, P. Experimental bench-scale study of residual biomass syngas desulfurization using ZnO-based adsorbents. *Energy Fuels* **2020**, *34*, 3326–3335. [CrossRef]
9. Zheng, X.; Zhang, G.; Yao, Z.; Zheng, Y.; Shen, L.; Liu, F.; Cao, Y.; Liang, S.; Xiao, Y.; Jiang, L. Engineering of crystal phase over porous MnO₂ with 3D morphology for highly efficient elimination of H₂S. *J. Hazard. Mater.* **2021**, *411*, 125180. [CrossRef]
10. Hatunoglu, A.; Dell'Era, A.; Del Zotto, L.; Di Carlo, A.; Ciro, E.; Bocci, E. Deactivation model study of high temperature H₂S wet-desulfurization by using ZnO. *Energies* **2021**, *14*, 8019. [CrossRef]
11. Castillo-Villalón, P.; Ramírez, J.; Cuevas, R.; Vázquez, P.; Castañeda, R. Influence of the support on the catalytic performance of Mo, CoMo, and NiMo catalysts supported on Al₂O₃ and TiO₂ during the HDS of thiophene, dibenzothiophene, or 4,6-dimethyldibenzothiophene. *Catal. Today* **2016**, *259*, 140–149. [CrossRef]
12. Wang, G.; Chen, G.; Xie, W.; Wang, W.; Bing, L.; Zhang, Q.; Fu, H.; Wang, F.; Han, D. Three-dimensionally ordered macroporous bulk catalysts with enhanced catalytic performance for thiophene hydrodesulfurization. *Fuel Process. Technol.* **2020**, *199*, 106268. [CrossRef]
13. Galindo-Ortega, Y.I.; Infantes-Molina, A.; Huirache-Acuña, R.; Barroso-Martín, I.; Rodríguez-Castellón, E.; Fuentes, S.; Alonso-Nuñez, G.; Zepeda, T.A. Active ruthenium phosphide as selective sulfur removal catalyst of gasoline model compounds. *Fuel Process. Technol.* **2020**, *208*, 106507. [CrossRef]
14. Chen, G.; Xie, W.; Li, Q.; Wang, W.; Bing, L.; Wang, F.; Wang, G.; Fan, C.; Liu, S.; Han, D. Three-dimensionally ordered macro–mesoporous CoMo bulk catalysts with superior performance in hydrodesulfurization of thiophene. *RSC Adv.* **2020**, *10*, 37280–37286. [CrossRef]
15. Tang, M.; Wang, W.; Zhou, L.; Zhang, Y.; Li, X. Reactive adsorption desulfurization of thiophene over NiMo/ZnO, a new adsorbent with high desulfurization performance and sulfur capacity at moderate temperature. *Catal. Sci. Technol.* **2019**, *9*, 6318–6326. [CrossRef]
16. Prajapati, Y.N.; Verma, N. Fixed bed adsorptive desulfurization of thiophene over Cu/Ni-dispersed carbon nanofiber. *Fuel* **2018**, *216*, 381–389. [CrossRef]
17. Shi, Q.; Wu, J. Review on sulfur compounds in petroleum and its products: State-of-the-art and perspectives. *Energy Fuels* **2021**, *35*, 14445–14461. [CrossRef]
18. Liu, Y.; Liao, J.; Chang, L.; Bao, W. Ag modification of SBA-15 and MCM-41 mesoporous materials as sorbents of thiophene. *Fuel* **2021**, *311*, 122537. [CrossRef]
19. Moosavi, E.S.; Dastgheib, S.A.; Karimzadeh, R. Adsorption of thiophenic compounds from model diesel fuel using copper and nickel impregnated activated carbons. *Energies* **2012**, *5*, 4233–4250. [CrossRef]
20. Saha, B.; Vedachalam, S.; Dalai, A.K. Review on recent advances in adsorptive desulfurization. *Fuel Process. Technol.* **2021**, *214*, 106685. [CrossRef]
21. Dehghan, R.; Anbia, M. Zeolites for adsorptive desulfurization from fuels: A review. *Fuel Process. Technol.* **2017**, *167*, 99–116. [CrossRef]
22. Zhang, D.; Yang, R.T. Superior silver sorbents for removing 2-vinyl thiophene from styrene by π-complexation. *Ind. Eng. Chem. Res.* **2019**, *58*, 1769–1772. [CrossRef]
23. Song, H.; Cui, X.; Song, H.; Gao, H.; Li, F. Characteristic and adsorption desulfurization performance of Ag–Ce bimetal ion-exchanged Y zeolite. *Ind. Eng. Chem. Res.* **2014**, *53*, 14552–14557. [CrossRef]
24. Yang, R.T.; Takahashi, A.; Yang, F.H. New sorbents for desulfurization of liquid fuels by π-complexation. *Ind. Eng. Chem. Res.* **2001**, *40*, 6236–6239. [CrossRef]
25. Takahashi, A.; Yang, F.H.; Yang, R.T. New sorbents for desulfurization by π-Complexation: Thiophene/benzene adsorption. *Ind. Eng. Chem. Res.* **2002**, *41*, 2487–2496. [CrossRef]

26. Hernández-Maldonado, A.J.; Yang, R.T. Desulfurization of liquid fuels by adsorption via π complexation with Cu(I)−Y and Ag−Y zeolites. *Ind. Eng. Chem. Res.* **2003**, *42*, 123–129. [CrossRef]

27. Oliveira, M.L.M.; Miranda, A.A.L.; Barbosa, C.M.B.M.; Cavalcante, C.L.; Azevedo, D.C.S.; Rodriguez-Castellon, E. Adsorption of thiophene and toluene on NaY zeolites exchanged with Ag(I), Ni(II) and Zn(II). *Fuel* **2009**, *88*, 1885–1892. [CrossRef]

28. Zhang, Z.Y.; Shi, T.B.; Jia, C.Z.; Ji, W.J.; Chen, Y.; He, M.Y. Adsorptive removal of aromatic organosulfur compounds over the modified Na-Y zeolites. *Appl. Catal. B Environ.* **2008**, *82*, 1–10. [CrossRef]

29. Lin, L.; Zhang, Y.; Zhang, H.; Lu, F. Adsorption and solvent desorption behavior of ion-exchanged modified Y zeolites for sulfur removal and for fuel cell applications. *J. Colloid Interface Sci.* **2011**, *360*, 753–759. [CrossRef]

30. Han, X.; Li, H.; Huang, H.; Zhao, L.; Cao, L.; Wang, Y.; Gao, J.; Xu, C. Effect of olefin and aromatics on thiophene adsorption desulfurization over modified NiY zeolites by metal Pd. *RSC Adv.* **2016**, *6*, 75006–75013. [CrossRef]

31. Liao, J.; Wang, W.; Xie, Y.; Zhang, Y.; Chang, L.; Bao, W. Adsorptive removal of thiophene from benzene by NaY zeolite ion-exchanged with Ce(IV). *Sep. Sci. Technol.* **2012**, *47*, 1880–1885. [CrossRef]

32. Sandoval-Díaz, L.-E.; González-Amaya, J.-A.; Trujillo, C.-A. General aspects of zeolite acidity characterization. *Microporous Mesoporous Mater.* **2015**, *215*, 229–243. [CrossRef]

33. Zu, Y.; Qin, Y.; Gao, X.; Mo, Z.; Zhang, L.; Zhang, X.; Song, L. Mechanisms of thiophene conversion over the modified Y zeolites under catalytic cracking conditions. *J. Fuel Chem. Technol.* **2015**, *43*, 862–869.

34. Zu, Y.; Hui, Y.; Qin, Y.; Zhang, L.; Liu, H.; Zhang, X.; Guo, Z.; Song, L.; Gao, X. Facile fabrication of effective Cerium(III) hydroxylated species as adsorption active sites in CeY zeolite adsorbents towards ultra-deep desulfurization. *Chem. Eng. J.* **2019**, *375*, 122014. [CrossRef]

35. Lee, D.; Ko, E.-Y.; Lee, H.C.; Kim, S.; Park, E.D. Adsorptive removal of tetrahydrothiophene (THT) and tert-butylmercaptan (TBM) using Na-Y and AgNa-Y zeolites for fuel cell applications. *Appl. Catal. A-Gen.* **2008**, *334*, 129–136. [CrossRef]

36. Mo, Z.; Qin, Y.; Zu, Y.; Wang, H.; Zhang, X.; Song, L. Effect of content of cerium ion on Bronsted-acid-catalyzed reaction of thiophene over CeY zeolite studied by in situ FTIR spectroscopy. *Chemistryselect* **2019**, *4*, 13034–13044. [CrossRef]

37. Zu, Y.; Guo, Z.; Zheng, J.; Hui, Y.; Wang, S.; Qin, Y.; Zhang, L.; Liu, H.; Gao, X.; Song, L. Investigation of Cu(I)-Y zeolites with different Cu/Al ratios towards the ultra-deep adsorption desulfurization: Discrimination and role of the specific adsorption active sites. *Chem. Eng. J.* **2020**, *380*, 122319. [CrossRef]

38. Liu, X.J.; Yi, D.Z.; Cui, Y.Y.; Shi, L.; Meng, X. Adsorption desulfurization and weak competitive behavior from 1-hexene over cesium-exchanged Y zeolites (CsY). *J. Energy Chem.* **2018**, *27*, 271–277. [CrossRef]

39. Zu, Y.; Zhang, C.; Qin, Y.; Zhang, X.; Zhang, L.; Liu, H.; Gao, X.; Song, L. Ultra-deep adsorptive removal of thiophenic sulfur compounds from FCC gasoline over the specific active sites of CeHY zeolite. *J. Energy Chem.* **2019**, *39*, 256–267. [CrossRef]

40. Li, H.; Han, X.; Huang, H.; Wang, Y.; Zhao, L.; Cao, L.; Shen, B.; Gao, J.; Xu, C. Competitive adsorption desulfurization performance over K-Doped NiY zeolite. *J. Colloid Interface Sci.* **2016**, *483*, 102–108. [CrossRef]

41. Song, H.; Wan, X.; Dai, M.; Zhang, J.; Li, F.; Song, H. Deep desulfurization of model gasoline by selective adsorption over Cu–Ce bimetal ion-exchanged Y zeolite. *Fuel Process. Technol.* **2013**, *116*, 52–62. [CrossRef]

42. Rui, J.; Liu, F.; Wang, R.; Lu, Y.; Yang, X. Adsorptive desulfurization of model gasoline by using different Zn sources exchanged NaY zeolites. *Molecules* **2017**, *22*, 305–317. [CrossRef] [PubMed]

43. Zhou, C.Y.; Alshameri, A.; Yan, C.J.; Qiu, X.M.; Wang, H.Q.; Ma, Y.N. Characteristics and evaluation of synthetic 13X zeolite from Yunnan's natural halloysite. *J. Porous Mater.* **2013**, *20*, 587–594. [CrossRef]

44. Yue, R.; Shuai, C.; Liu, C.; Lu, B.; Xu, J.; Wang, J.; Liu, G. Synthesis, characterization, and thermoelectric properties of a conducting copolymer of 1,12-bis(carbazolyl)dodecane and thieno [3,2-b] thiophene. *J. Solid State Electrochem.* **2012**, *16*, 117–126. [CrossRef]

45. Song, Y.; Peng, B.; Yang, X.; Jiang, Q.; Liu, J.; Lin, W. Trail of sulfur during the desulfurization via reactive adsorption on Ni/ZnO. *Green Energy Environ.* **2021**, *6*, 597–606. [CrossRef]

46. Mills, P.; Korlann, S.; Bussell, M.E. Vibrational study of organometallic complexes with thiophene ligands: Models for adsorbed thiophene on hydrodesulfurization catalysts. *J. Phys. Chem. A* **2001**, *105*, 4418–4429. [CrossRef]

47. Liao, J.-J.; Bao, W.-R.; Chang, L.-P. An approach to study the desulfurization mechanism and the competitive behavior from aromatics: A case study on CeY zeolite. *Fuel Process. Technol.* **2015**, *140*, 104–112. [CrossRef]

48. Velu, S.; Song, C.; Engelhard, M.H.; Chin, Y.-H. Adsorptive removal of organic sulfur compounds from jet fuel over K-exchanged NiY zeolites prepared by impregnation and ion exchange. *Ind. Eng. Chem. Res.* **2005**, *44*, 5740–5749. [CrossRef]

49. Zhao, S.; Mo, Z.; Qin, Y.; Song, Y.; Shi, L.; Zhu, M.; Song, L.; Duan, L. Adsorption, desorption and conversion of methylthiophene on HY zeolite. *J. Fuel Chem. Technol.* **2015**, *43*, 614–618.